

A2Cflow models's Simulation and Analysis of Airflow around Single Building

Jenny S-N Hui and Jen-Hsin Teng
Research and Development Center, Central Weather Bureau, R. O. C.

Abstract

A three-dimensional numerical atmospheric modeling system, Atmosphere to Computational Fluid Dynamics flow (A2Cflow), is used to study the airflow around a building. Both horizontal and vertical flow characteristics around a building with different building width-to-height ratio and boundary stability condition under 5 m/s westerlies winds are presented in this paper. The model simulations results capture most of the features, including the flow separation around building, reverse flow and recirculation region behind building. The major difference between the simulation results lies in the cavity region behind building. Two prominent symmetric vortexes are identified at the low pressure zone and stronger reversed flow is evident behind building for the simulation of larger building width. The cavity recirculation behind the building is considerably smaller and skewed for the simulation of smaller building width. Also, higher building is result in stronger lee wave downstream flow.

Also, the predications of the distance from the downstream edge of the building to the reattachment point at ground level along the vertical center-plane of the building associated with different Froude number (Fr) and building width-to-height (W/H) ratio by the model's result are discussed. It is apparent that the normalized reattachment length increases with Fr under stable condition, reaches a peak value in the region where Fr between 2 and 4, then slightly decreases and finally reaches a constant value under unstable condition. Strongest wind are develop around building when Fr equal to 3 which provide high kinetic energy for allowing the flow over the building and result of longer reattachment distance. Moreover, model's result show that the reattachment distance increased as the W/H ratio increased and varied when the boundary conditions changed. By comparing the model result with experiments from previous studies, good agreement is obtained. Key words: air flow around building, reattachment distance, A2Cflow

1. Introduction

Studying of airflow transportation and dispersion pattern around buildings is a challenging task due to the complex flow induced by the surface-mounted, interfered by adjacent buildings, and the geometrical variations of buildings. Also, the properties of buildings airflows, such as wind profile, temperature, pressure and turbulence are determined by the supply air, thermal buoyancy, geographic and weather conditions.

In this study, the A2Cflow model is used to simulate the airflow around building. Several cases of the numerical simulation of airflow with different approaching boundary instability condition and building width-height ratio around the building are carried out to estimate the influences on the simulated results. The model predicts the airflow around building and the length of the primary recirculation zone (i.e. the distance from the downstream edge of the building to the reattachment point at ground level along the vertical center-plane of the building) associated with different Froude number and building scale. Section 2 of this paper describes the A2Cflow model and simulations setting used in this study. Section 3 presents the result of the horizontal and vertical wind filed around the building while section 4 shows the variation of reattachment distance behind building. The summary is given in section 5. The objective of the work is to first understand

the complex flow patterns that result from the interaction of the wind with single building under various boundary conditions and evaluate the performance of the model resulted comparing with literature. Then, the predicated result by the numerical modeling can apply to the air pollution issues, environmental assessment for site planning and urban planning when making decisions.

2. Model

The basic equations of A2Cflow are described in details by Yamada and Bunker (1988, 1989) and model detailed can be obtained from the web-site <http://ysasoft.com/about/company.htm>; only a summary is given here. Five primitive equations are solved for ensemble average variable: three wind components, potential temperature, and mixing ratio of water vapor (Yamada and Bunker 1988). In addition, two primitive equations were solved for turbulence that the turbulence kinetic energy and length scale are solved based on the level 2.5 Mellor-Yamada second moment turbulence-closure model (1974, 1982). The Highly Simplified Marker and Cell (HSMAC) method (Hirt and Cox, 1972) non-hydrostatic pressure computation is adopted and the terrain-following vertical coordinate system is used to treat surface boundary conditions accurately. The model has been extensively used for meteorological and air-quality studies that indicate the

models' results are in good agreement with observations in wind-tunnel experiments and can be applied under a variety of actual atmospheric conditions.

The numerical simulations shown in this study is designed to model the dynamical flow field around a single building. Two domains are computed for each steady state simulation under zero-terrain to neglect the effect of topography. The horizontal grid spacing is 6m and 12m for the inner and outer domains respectively. The vertical grid spacing is 4m for 80m above ground and increased with height up to 200m for both domains. A total number of grid points are $98 \times 100 \times 30$ for the fine mesh and $64 \times 62 \times 30$ for the coarse mesh. We adapt the non-hydrostatic pressure and steady state condition options. All cases are carried out for a period of one hour simulation for maintaining in steady-state condition.

For Section 3, the model simulations of airflow with different building width-height ratio of the building are carried out. Rectangular building is set with fixed length ($L = 48\text{m}$), but various with width ($W = 48\text{m}, 96\text{m}, 144\text{m}, \text{and } 240\text{m}$) and height ($H = 30\text{m}, 40\text{m}, 50\text{m}$ and 60m). The simulations are computed with a uniform initial prevailing wind of 5m/s from west to east and normal to the building surface. Three different boundary stability condition with $0.001, 0.003, 0.005 \text{ } ^\circ\text{C}/\text{m}$ potential temperature gradient averaged over a day which commonly occurs at normal atmospheric conditions are used for understanding the effect of stability condition to the flow pattern around building.

For section 4, several cases of the airflow simulation with different approaching boundary instability condition are conducted to discuss the variation of flow reattachment point as a function of Froude number. As the models predict results are then compared with previous CDF model and towing-tank studies presented in Snyder (1994), Zhang et al. (1996) and William (2001), the same parameters with uniform initial prevailing wind (U) of 7m/s and 60m cubical building (H) is set to ensure the flow field in the vicinity of the building revealed by previous studies could be also adequately modeled by A2Cflow model.

3. Flow characteristics around single building

At horizontal plane, the approaching winds collided with the building wall which resulted in increasing dynamic pressure on the windward side while decreasing pressure on the leeward side of the building. The flows are separated from the building and are accelerated at the both upwind and downwind corners. Figure 1 show the wind distribution in the horizontal plane at 10m above the ground for the simulation of 50m height building under $0.003 \text{ } ^\circ\text{C}/\text{m}$ stability condition. The major difference between the results lies in the cavity region behind building. In the case with large building width ($W=240\text{m}$), two prominent symmetric vortexes are identified at the low pressure zone and stronger reversed flow is evident about 180m behind the building (Fig 1.b). Then the flows near the northern and southern sides of the building formed a convergent zone. While in the case

with small building width ($W=48\text{m}$), the vortex cannot be clearly seen and reverse flow are rather weak (Fig 1.a). Also, weaker outflows parallel out behind the building. The simulation case of $30\text{m}, 40\text{m}, 50\text{m}$ and 60m building height also shows the same features. Similar flow pattern as $0.003 \text{ } ^\circ\text{C}/\text{m}$ stability condition is found for the $0.005 \text{ } ^\circ\text{C}/\text{m}$ and $0.001 \text{ } ^\circ\text{C}/\text{m}$ stability condition (figure not shown).

At vertical cross section, the wind dams up against the upwind side of the building which result in develop a high pressure area and increase wind speed along the upper edge and sides of the building. Small vortex or eddy currents are created aloft of these windward edges. There is a slightly increase of pressure and thus wind speed along the downwind portion of the roof and sides. The wind then moves past the back of the building and a huge low pressure area is created that causes the wind to curl in to fill the void.

Figure 2 show the x-z vertical center-plane wind field across the building for the simulations case of 30m and 60m building height. It is concluded that the boundary flow direction change about $1H$ in front of the building and the elevated levels of the accelerated flow extended about $2.0H$ upstream of the building, where H is the building height (Fig 2). Higher building and larger building width are also result in stronger lee wave downstream flow. In the case with small building width ($W=96\text{m}$), the cavity circulation behind the building is considerably smaller and skewed (Fig 2 a). While for the case with $W=240\text{m}$ building width, the recirculation zone is larger and circular (Fig 2 d). The simulation of 30m building height result show that the length of the leeward recirculation zone is $2.67H$ and $6.9H$, for $W=48\text{m}$ and 240m building width respectively (Figure not shown). This feature is the result of difference area occupied and wind speed for the upward and downward motions in the cavity region behind building. For the case of small building width, the area and strength of upward motion is small and weak. While in the case of large building width, the occupied area of strong upward and downward motion is larger that strong eddy winds downwind of the building develop. Also, stronger and broader area extend of downstream flow is found. This notice feature of leeward recirculation zone and the distance from the downstream edge of the building to the reattachment point at ground level along the vertical center-plane of the building is shown in the models result. More discussion is focused on the reattachment point at next section for different building's width-to-height ratio and boundary stability condition.

From the preliminary result, the A2Cflow model is able to simulate the flow characteristics around building that capture most of the features among different building width-height ratio, including the flow separation, reverse and recirculation zone. The details of airflow and pressure change around building are also revealed at previous studies William 2001; Yamada 2004.

4. Reattachment distance behind building

(a) Varies with boundary stability condition (as a

It is commonly known that the Froude number ($Fr = \frac{U}{NH}$, where U is the flow speed, N is the Brunt-Vaisala frequency and H is the height of building) is used to describe the flow pattern over a building. If $Fr \ll 1$, the air in a stably stratified environment will flow around, not over the building and even the flow will be blocked. If $Fr \gg 1$, the air readily flows over the building with little lateral displacement. At this study, several cases of numerical simulation of airflow around a building are carried out to estimate the influence of boundary stability condition as a function of Fr to the reattachment point. For the given (U) and (H), Fr is only the function of stability. When Fr is small (large), it is in a stable (unstable) condition.

Figure 3 shows the comparison of the reattachment distance normalized by the building height as a function of Fr , with the towing-tank data and other two CDF (Computational Fluid Dynamics) model results. It is seen that the A2Cflow model can simulate well the change of reattachment point varied with the boundary stability condition. The change in reattachment point is in a good agreement with towing-tank, that the reattachment distance increases as Fr is small (from very stable to neutral condition) and maintains a constant reattachment distance while Fr is large (from unstable to very unstable condition). However, the model result tends to underestimate the reattachment point in comparison with towing-tank data and the two CDF models, especially in the regime where Fr is very small ($Fr \leq 2$). It is due to the coarse resolution (6m) in the model configuration that cannot be well resolved the flow near the sidewall of the recirculation zone behind the building. As we conduct another finer resolution (4m) simulations, the predicted reattachment points which are marked as solid circles shown at Fig 3 are compared favorably with the experimental data.

Moreover, a transition in the range of Fr from 2-4 reported by TEMPEST model in Zhang et al. 1996 is also seen in A2Cflow models results. Peak reattachment point is shown when Fr is equal to 3, then the reattachment distance gradually decreases and is nearly independent of Fr when Fr is greater than 4. The TEMPEST model also shows the features but tends to over-predict the recirculation region behind the building. However, these features can not be clearly identified in towing-tank data and HIGRAD model result from the figure that the reattachment point is independent when Fr is greater than 2. More discussion on the transition of reattachment distance is presented at section 4 (c).

Also we conducted another inflow wind 5m/s simulations to check how sensitive are the model results of reattachment distance to the inflow boundary wind conditions (Figure 4). Difference is shown among the two inflow wind conditions that the higher the wind speed, the shorter the reattachment distance will be.

Once more, the results show that a transition of reattachment distance exists when Fr between 2 and 4.

(b) Varies with building width-to-height ratio

Previous studies from (Snyder and Lawson, 1994; Brown et al., 2001) which conducted wind tunnel measurements to find the relationship between building width-to-height ratio and reattachment distance. However, the results show significant differences between them. Here, several cases of A2Cflow flow model simulations are carried out to estimate the influence of building scale on the reattachment distance. Figure 5 shows the variation of normalized reattachment distance with different W/H under 0.001°C/m, 0.003°C/m and 0.005°C/m boundary stability conditions for the simulation cases of 30m, 40m, 50m and 60m building heights respectively. Preliminary results show that reattachment distance increases as the W/H ratio increases and is nearly independent when W/H is greater than 6. Also, the reattachment distance increases under the 0.005°C/m (more stable) boundary stability condition while it decreases under 0.001°C/m (more unstable) boundary stability condition. Also, higher buildings result in shorter reattachment distances. It is the result of stronger downward motions in the cavity region behind the building that the airflow meets to the ground at the closest point. The modeled results show that the reattachment distance is sensitive to the building configuration and inflow boundary conditions. This might explain why the reattachment distance varies in different wind tunnel experiments and model results.

(c) Discussion on the change of reattachment distance

From the preliminary results in the simulation, it is indicated that the more stable the air, the higher its natural oscillation frequency and as a result the increase of reattachment distance is shown. Under more unstable conditions, the air flow is free to climb up along the upwind side of the building and reach a constant reattachment distance. A transition zone of reattachment distance is identified in the region of Fr from 2-4 (from stable to unstable condition). Furthermore, the Fr between 2 and 4 often happens in actual atmosphere that Fr will be nearly equal to 3 in the nighttime stable boundary layer, and larger Fr at daytime. So, more discussion is needed to focus in the region when Fr between 2 and 4 for understanding the complex airflow around the building. Three points (i), (ii) and (iii) shown in figure 3 for $Fr = 2.5, 3.0$ and 7.1 respectively are selected for understanding the flow differences among them. Point (i) and (iii) have nearly the same reattachment distance but under different stability conditions while point (ii) is the maximum point of reattachment distance. Figure 6 shows the horizontal wind distributions of 36m and 60m above ground for the three-selected points. Strongest wind flow around the building exists under point (ii) condition that provides more kinetic energy to flow over the building and extend to longer reattachment points.

5. Summary

Three-dimensional atmospheric prediction combined with CFD model, A2Cflow, is used to study the airflow around building. The model simulations results capture most of the features, including the flow characteristics around building, the variation of the flow reattachment point and compare favorably with the experimental data. Several cases of numerical simulation of airflow around a building are carried out to estimate the influence of boundary stability condition (as a function of Froude number) and building's width /height scale to the model resulted. Similar flow pattern is found for the $0.001^\circ\text{C}/\text{m}$, $0.003^\circ\text{C}/\text{m}$ and $0.005^\circ\text{C}/\text{m}$ boundary stability condition while the geometry of building has significant effect on the wind distribution and the strength of eddies downwind behind building. Most of the turbulence is on the downwind side of the building. From all the simulations, it can conclude that the flow of (i) $1.0H$ area in front of the building experience the change of the wind direction (ii) $2.0H$ directly above and windward exhibit localized wind speed increases and changes of direction as the wind builds up and flows around and over the building and (iii) $7.0H$ of a eddy recirculation zone develops behind building.

The reattachment distance varied when the inflow boundary conditions and building width-to-height ratios changed. For example, reattachment distance increased as the W/H ratio increased. Also, the reattachment length increases with Fr under stable condition, reaches a peak value, then decreases and finally reaches a constant value under unstable condition. For the studied case, the strongest wind flow over the building result of maximum reattachment distance when Fr equal to 3. Also, faster winds increase the turbulence but decrease the length of the reattachment distance. The building width-to-height ratio, combined with the wind speed and stability condition will determine both the amount of turbulence and the length of area with reduced wind speed downwind of the building. In further, there is a need for high-quality data to evaluate the models performance especially for the transition zone of reattachment distance and discover the important of underlying physical process for understanding and prediction of the complex airflow around buildings.

References

- Hirt, C.W. and Cook, J.L., 1972: Calculating Three Dimensional Flows around Structures and over Rough Terrain, *Journal of Computational Physics*, Vol. 10, 324-340.
- Snyder, W. & R. Lawson, Jr., 1994: Wind-tunnel measurements of flow fields in the vicinity of buildings. *8th AMS J. Conf. on Appl. of Air Poll. Met. with AWMA*, Nashville, TN, 244-250.
- William S. Smith, J. M. Reisner, and C. Y. J. Kao, 2001: Simulations of flow around a cubical building: comparison with towing-tank data and assessment of radiatively induced thermal effects. *Atmospheric Environment*.

Yamada and Bunker, 1988: Development of a nested grid, second moment turbulence closure model and application to the 1982 ASCOT Brush Creek data simulation, *JAM*.

Yamada, T. and S. Bunker, 1989: A numerical model study of nocturnal drainage flows with strong wind and temperature gradients, *J. Appl. Meteor.*, 28: 545-554.

Yamada, T., 2004: Merging CFD and Atmospheric Modeling Capabilities to Simulate Airflows and Dispersion in Urban Areas. *Computational Fluid Dynamics Journal*, 13(2):47, 329-341.

Zhang, Y. Q., Arya S. P., Snyder, W. H., 1996: A comparison of numerical and physical modeling of stable atmospheric flow and dispersion around a cubical building. *Atm. Env.*, 30, 1327-1345.

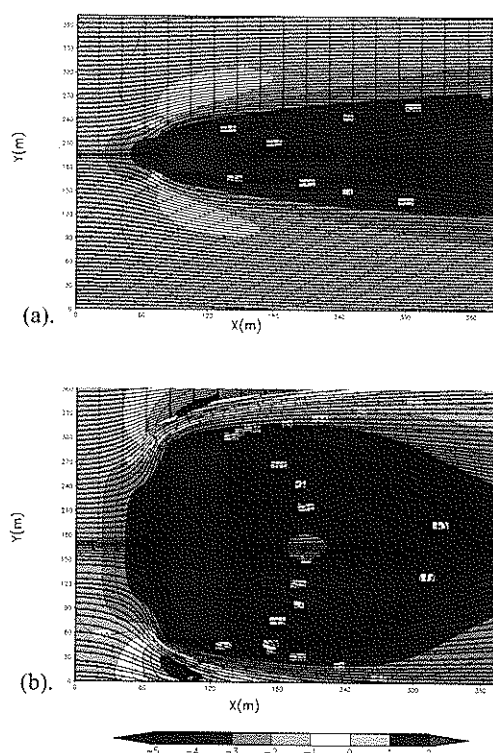


Figure 1 Wind distribution at 10m above the ground under $0.003^\circ\text{C}/\text{m}$ potential temperature gradient simulations for building length 48m (L), height 50m(H) and width (a) 48m (W), (b) 240m (W).

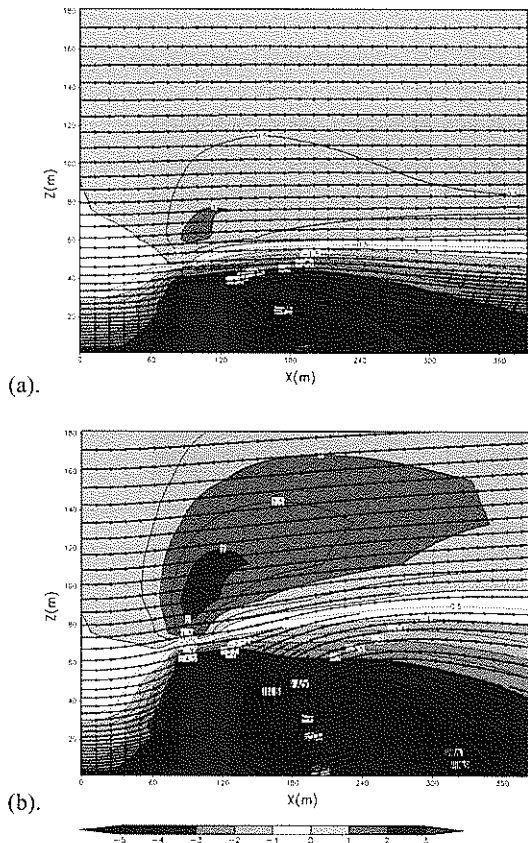


Figure 2 Wind distributions in the vertical cross section along a centerline under $0.003 \text{ } ^\circ\text{C/m}$ potential temperature gradient simulations for (a) 48 (L) x 96m (W) x 30m (H), (b) 48 (L) x 240m (W) x 60m (H) building.

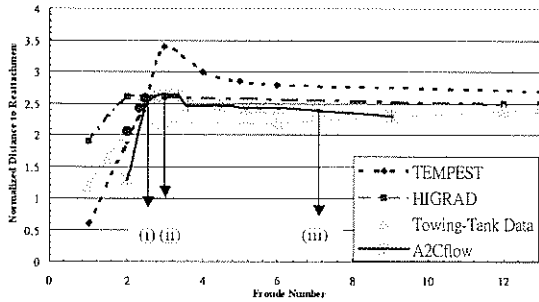


Figure 3 Comparison of the A2Cflow predicted normalized reattachment distance as a function of Froude number with previous studies. Towing-tank data and RANS models result (TEMPEST) are from Zhang et al., 1996, and LES model result (HIGRAD) is from William et al., 2001.

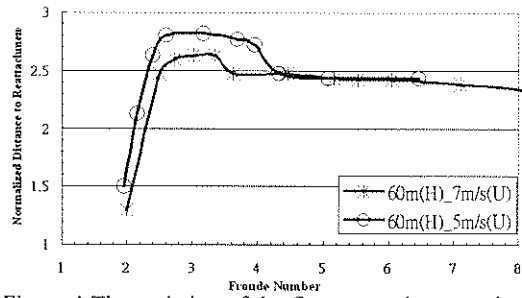


Figure 4 The variation of the flow reattachment point as a function of Fr for 60 m cubical building with 5m/s (circle symbol with purple line) and 7m/s (cross symbol with green line) wind condition.

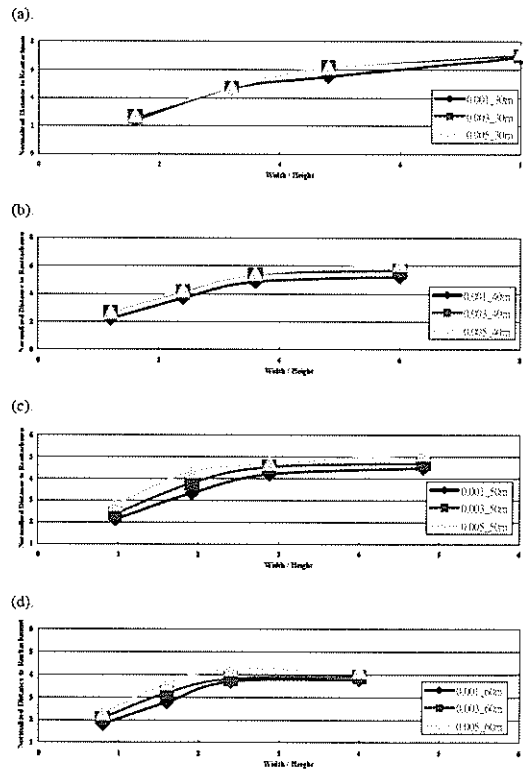


Figure 5 The variation of the flow reattachment point with different building width-to-height ratio for (a) 30 m, (b) 40m, (c) 50m and (d) 60m building height under 0.001, 0.003, 0.005 $^\circ\text{C/m}$ potential temperature gradient.

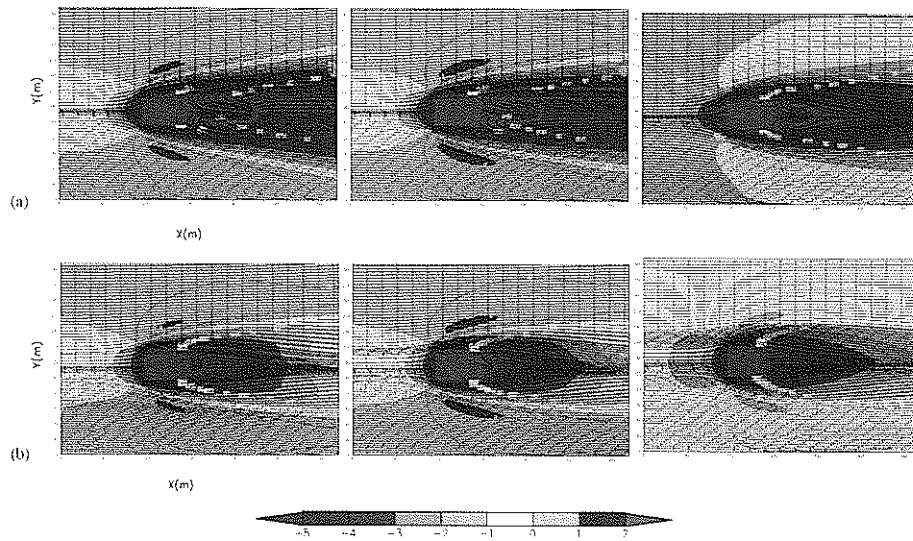


Figure 6 Wind distributions at (a) 36m and (b) 60m above the ground for the 60m cubical building simulations case with 7m/s inflow boundary. The left, center and right panels are under the stability condition that show in figure 3 for point (i), (ii) and (iii) respectively.